

EFFECT OF HEAVY LIQUID FUEL TEMPERATURE ON THE TWIN FLUID ATOMIZATION CHARACTERISTICS

SHABANA H. WILSON S.A. SYAM A.R.
Mechanical Power Engineering Dept.
Faculty of Engineering , Menoufia University
Shebin El-Kom , Egypt.

تأثير درجة حرارة الوقود السائل الثقيل على خصائص التذير للمزرات ثنائية المائع الخلاصة

يعتبر الوقود السائل الثقيل (المزوت) نظراً لخصائصه وفرة المتاح منه في مصر أكثر أنواع الوقود الهيدروكربوني استخداماً في عمليات الاحتراق في الأفران. وتوقف جودة الاحتراق واستقراره على جودة عملية تدمير الوقود من حيث قطر القطرات وسرعة انتشارها واختلاطها بالهواء داخل حيز الاحتراق. وحيث أن خصائص التذير تتوقف بشكل مباشر على الخواص الطبيعية للوقود مثل الكثافة واللزوجة والتوتر السطحي التي هي بدورها دوال في درجة حرارة الوقود المذير، لذلك فإن دراسة عملية تدمير الوقود الثقيل - الذي عادة ما يذير عند درجات حرارة أعلى من المعتادة لأنواع الوقود السائل الأخرى - تتطلب دراسة تأثير ارتفاع درجة حرارة الوقود على مواصفات التذير وهذا ما يتناوله هذا البحث.

البحث عبارة عن دراسة عملية ونظرية لأثر درجة حرارة الوقود السائل الثقيل على سلوك القطرات المتكونة نتيجة التذير وتوزيعها وسرعة انتشارها في الهواء الجوي.

استخدم في القياسات العملية أشعة الليزر (laser doppler analyser) لسرعة استجابتها العالية ولما لها من قدرة على قياس قطر القطرة وسرعتها في آن واحد مما يعكس بصورة إيجابية عى دقة القياسات.

في الجزء النظري من البحث تم تطوير نموذج رياضي لدراسة السريان ثنائي الوجه (وقود- هواء) وذلك باعتبار أن سريان الهواء بالمذير مستقر، ثلاثي البعد، قابل للإلتصاف واضطرابي. وكذلك تم حل معادلات الحركة والطاقة للقطرات مع الأخذ في الاعتبار التأثير بين الهواء والوقود. تم تعديل ثوابت معادلة لوفيفر التجريبية لحساب القطر المميز للقطرات (D_{32}) وذلك باستخدام النتائج العملية الحالية لتناسب الوقود السائل الثقيل.

بين البحث أنه كلما زادت درجة حرارة الوقود كلما قل تبعاً لذلك قطر القطرات المذرة وسرعة انتشارها. كذلك بين البحث تطابق مقبول بين القياسات العملية والقيم المناظرة المحسوبة من النموذج الرياضي المقترح.

ABSTRACT

The effect of heavy liquid fuel properties on the atomization characteristics is introduced. Detailed measurements of the drop size and the velocity distribution were obtained for a twin fluid externally mixing atomizer. The Phase Doppler Particle Analyzer is used in the current measurements. The simultaneous measurement of drop size and velocity was the major importance in accurately describing the changes in the local drop size distributions and mass flux. Result

shows a noticeable decrease in droplet size distribution and the corresponding droplets velocity with increasing fuel temperature. A mathematical model was developed to predict the atomization process. The stochastic separated flow model (SSF) as well as modified interaction mechanism between the two phases of the spray were taken into account to improve the capabilities of the prediction method.

INTRODUCTION

The atomization of liquid fuels and the mixing process plays decisive role in governing the combustion, stability, heat release and consequently the combustion efficiency in general. While for heavy liquid fuels as special case (which is considered as the most economical hydrocarbon fuel), the properties i.e., density, viscosity and surface tension affect directly upon the atomization behaviour. Consequently, the required atomization degree can be achieved.

Several experimental works [1, 2, 3] were made using different types of atomizers and fuels with different properties (viscosity in the range of 0.0013 to 0.0183 Pa.s). An empirical formula representing the change of Sauter Mean Diameter (D_{32}) with respect to fuel properties and operating conditions was proposed by Lefebvre [1]. The correlation was found to be good agreement with the experimental data for the light fuel viscosity than that of the heavy one. So a modified correlation for specifically heavy liquids is needed. In the present work steady flow twin fluid atomization with externally mixing process was used. The atomizer design facilitates the variation of the discharge area of fuel orifice. In addition, a swirl generator in the air side was used in order to give the atomizing air a tangential velocity component before the mixing process. In the twin fluid atomizers, the nozzle geometry as well as the operating conditions (fuel pressure, air pressure and the ambient conditions) plays an important role for governing the atomization characteristics. In addition the physical properties of the liquid fuel in general and in heavy liquid fuel as special case affects directly upon the spray behaviour. The changes of the fuel properties with temperature were taken into consideration with reasonable working temperature range (40-90°C). The effect of the injection pressure and air pressure on the atomizing degree was taken into consideration. The ambient conditions for the spray were kept constant at the atmospheric condition.

In the theoretical field, different works [5-11] developed different mathematical models. In the present work, the stochastic separated flow model is used to predict the spray characteristics. The modified technique is used to calculate the two phases (gas-liquid) interaction.

EXPERIMENTAL WORK

A schematic diagram of the experimental apparatus is shown in Fig. 1. It consists mainly of an atomizer (2) mounted on a chamber (1) with two opposite glass walls. The fuel system consists from a helical fuel pump (8), fuel tank (5) provided with an electrical heater (6). A traverse mechanism to allow 2D measurements inside the spray zone has been provided. Suction system (14) with variable suction velocity to prevent any clouds caused by the evaporation of small droplets or the population of the very small ones inside the measuring zone was

constructed. Several measuring devices were mounted in different measuring points to adjust, control and measure the desired operating conditions. Figure 2 represents the design details of the atomizer employed in the present work. Two separate paths for air and fuel are used to ensure externally mixing process. A swirl generator with swirl angle 30° is mounted inside the air path. This leads to enhance the atomization process. The fuel nozzle inner diameter is 1 mm. It is provided with internal and adjustable needle. So the desired effective nozzle area can be obtained. It can be adjusted between zero and the maximum area corresponding to the nozzle diameter. In the present work, the experiments were carried out with maximum nozzle area ($\frac{\pi}{4} d_0^2$). The air cup with internal diameter 5 mm was used. A brief description of the experimental work is given. Fuel is heated to the desired temperature before entering the fuel pump. The fuel pressure is regulated to the desired pressure via bypass valve. The fuel is then flow through the thermally isolated fuel line to the injector. The fuel temperature is recorded at the entrance to the atomizer. The fuel is then injected from the fuel nozzle (1 mm diameter) forming very dense spray with long solid core length and narrow cone angle. The compressed air valve is opened and regulated to the desired quantity. The air flow rate is measured via the orifice meter and the air pressure is recorded at the entrance to the atomizer. By controlling the air pressure, the final required spray characteristics can be achieved.

The He-Ne Phase/Doppler Particle Analyzer (P/DPA) is used to measure the local droplets size distribution, velocity distribution and fuel concentration simultaneously. The dynamic measuring range was 35, so it covers a reasonable range of droplet size and velocity. The scattering light from the droplets crossing the laser beams intersection, is recorded and processed. A very high sampling rate data acquisition system is used to overcome the local frequency of the spray droplets.

The experiments were conducted in different operating modes. Fig. 3 represents the change of the fuel viscosity and density with temperature. The decay of surface tension with temperature for the fuel used is shown also in Fig. 4. The other properties of the fuel are as follows.

- Fuel type : furnaces mazot.
- Flash point (bensky martin) : 94°C min - 132°C max.
- Pouring point : 29°C min - 43°C max.
- Sulphur% (by weight) : 0.65 min - 2.64 max

Figure 5 represents typical output result from the data acquisition system of the P/DPA. The figure shows the simultaneous droplets size and velocity distribution. Some important statistical quantities for the droplets population are obtained. These quantities are the average droplets diameter, the most probable, the Sauter mean diameter and others. On the other hand the average droplets velocity and the corresponding r.m.s. are calculated and displayed as shown in the figure.

Figure 6 shows the effect of fuel temperature on the Sauter mean diameter of the droplets along the spray axis. Increasing the temperature, the droplets tends to be smaller. The initial droplets formed in the spray represented by D_{32} depends mainly upon the Weber number. So decreasing the viscosity and surface tension with temperature leads to increase in Weber (We) and Reynolds number (Re) and finally decrease the initial D_{32} . On the contrary the droplets initial velocity increases with increasing the fuel temperature as shown in Fig. 7 but with narrow changing range. This can be attributed to the decrease of the fuel density with increasing the fuel temperature as shown in Fig. 3, on which the fuel jet velocity is proportional to the reciprocal of the square root of the density. The following empirical form representing the axial spray velocity was obtained.

$$U/U_0 = 5.12 (X/d_0)^{-0.48} \quad (1)$$

Form the dimensionless analysis, it has been shown that the basic drop size empirical formula for twin fluid atomizer can be represented by Lefebvre [1] correlation.

$$D_{32}/d_0 = (1+1/AF) [A We^B + C (We^{0.5}/Re)^D] \quad (2)$$

Where, A, B, C and D are correlation constants. By applying the present experimental data on the last equation, the following constants can be obtained

$$A = 0.012 \quad B = -0.5 \quad C = 0.52 \quad D = 0.5,$$

AF is the air to fuel ratio by mass = 8.5, other values can be used. ,

$$\text{and} \quad We = \rho_A U_R^2 d_0 / \sigma (t)$$

$$Re = \rho_L (t) U_R d_0 / \mu (t)$$

The change of the fuel properties with temperature is correlated as follows :

$$\sigma (t) = 0.0336 - 65.6E-6 (t-40) \quad t > 40 \text{ } ^\circ\text{C}$$

$$\rho (t) = 945 - 656 (t-20) \quad t > 20 \text{ } ^\circ\text{C}$$

$$\mu(t) = 8 \text{ Exp } (725/82.25 + t) \quad t > 40 \text{ } ^\circ\text{C}$$

The ability of equation (2) to correlate the values of D_{32} obtained, experimentally is illustrated in Fig. 8. The radial droplet size distribution at the spray cross section is shown in Fig. 9. It is clear from this figure the effect of the fuel temperature on decreasing the radial droplet size distribution. This can be attributed to the reduction in the initial droplet size distribution with respect to fuel temperature.

THEORETICAL WORK

The proposed mathematical model in the present work is based on the strongly coupled set of nonlinear partial differential equations. These are the continuity, momentum and energy equations for both gas and liquid phases. The two equations for turbulent flow (k- ϵ) are used also. The gas phase motion is considered as steady, 3D, compressible and turbulent flow.

Gas Phase Equations

According to the last assumptions, the conservation equations of continuity, momentum (3D) and the energy equations are employed to simulate the gas phase. The equation of state is used also to calculate the air density. The general form of the conservation for the continuum phase is as follows.

$$\frac{\partial}{\partial x} \rho U \phi + \frac{\partial}{\partial y} \rho V \phi + \frac{\partial}{\partial z} \rho W \phi = \frac{\partial}{\partial x} \Gamma_{\phi} \frac{\partial \phi}{\partial x} + \frac{\partial}{\partial y} \Gamma_{\phi} \frac{\partial \phi}{\partial y} + \frac{\partial}{\partial z} \Gamma_{\phi} \frac{\partial \phi}{\partial z} + S_{\phi} + S_{\phi L} \dots(3)$$

and $\rho = P / RT$

Where ϕ is any one of the dependent variables U,V,W, H,k and e. The effective diffusion coefficient is denoted by Γ_{ϕ} , S_{ϕ} and $S_{\phi L}$ are the source of ϕ from the gas phase and the liquid phase respectively. Detailed expressions for each dependent variable source term are listed in [12]. The finite volume, with iterative scheme is used to solve the elliptic flow in Eulerian domain. The physical domain is covered with 16x20x10 grid. The SIMPLEC [14] algorithm is used for more accurately calculating the pressure field and to accelerate the iteration procedure.

Liquid Phase Equations

The liquid phase which is the discontinuum phase, consists from the spray droplets. The droplets conservation equation can be written in Lagrangian form as follows.

$$dm_L U_L / dt = - C_D \rho_g A_L U_R^2 / 2 \quad (4)$$

Where.

$$C_D = 27 / Re^{0.84} \quad \text{for} \quad 0 < Re < 80 \quad \text{and}$$

$$C_D = 0.271 Re^{0.217} \quad \text{for} \quad 80 < Re < 10000$$

The conservation equation of energy can be put in the following form.

$$m_L C_{pL} (dT / dt) = A_L h (T_a - T_L) + L (dm_L / dt) \quad (5)$$

The rate of droplets temperature increase becomes as follows.

$$dT / dt = \left(\frac{3}{R_L C_{pL}} \right) \left[\left(\frac{h}{\rho_L} \right) (T_a - T_L) - \left(\frac{L Sh D_C}{2 R_L \rho_L} \right) \left(\frac{P_s}{R_v T_s} \right) \right] \quad (6)$$

where, h is the coefficient of heat transfer and it can be calculated from the Nusselt number according to the following correlation [15,16] :-

$$Nu = \beta 0.54 Re \quad \text{for} \quad 100 < Re < 100$$

$$Nu = \beta (2 + 0.6 Re^{1/2} Pr^{1/3}) \quad \text{for} \quad Re < 100$$

where β is a correction factor to consider the effect of mass transfer [17]

$$\beta = Z / (e^Z - 1)$$

and, $Z = - \left[C_{p_v} \left(\frac{dm}{dT} \right) / \pi D K Nu \right]$

For non evaporating droplets $\beta=1$

The Sherwood number (Sh) and the diffusion coefficient (D_c) required for solving equation 6 can be found from following relations [18] :-

$$Sh = 2 + 0.6 Re^{1/2} Pr^{1/3}$$

$$D_c = D_0 \left(\frac{T_s}{T_0} \right) \left(\frac{P_0}{P_s} \right)$$

Droplets Gas Phase Interaction

The effect of the droplets motion on the gas phase turbulence level appear as a pseudo turbulence shear stress [12] in the source term of the gas phase. This can be represented in the following tensor notation.

$$\tau_{ij,ps} = \mu_{ps} [(\partial U_i / \partial x_j) + (\partial U_j / \partial x_i)] \quad (7)$$

Where,

$$\mu_{ps} = 1.3 \rho_a \alpha R_L U_R$$

The effect of the gas phase on the droplets motion depends on the time interval over which the droplets interact with the randomly sampled gas phase velocity fluctuation. This is determined by the slip velocity and the droplet residence time within a turbulent eddy. The residence time is estimated as follows.

$$\tau_r = \tau \ln \left[1 - \frac{l}{\tau} U_R \right] \quad (8)$$

Where, τ is the droplets relaxation time = $(8/3) \rho_g R_L / (C_D U_R)$

and l is the turbulence length scale,

$$l = C_\mu^{3/4} k^{3/2} / \epsilon$$

$$C_\mu = 0.09$$

The eddy life time is estimated form the following expression;

$$\tau_e = l / u' = l / \left(\frac{3}{2} k \right)^{1/2}$$

The droplets turbulence interaction time is considered as follows :-

$$\tau_{int} = \min (\tau_r - \tau_e)$$

The instantaneous turbulence velocity of the air field is used in the calculation of the drag force. This can be represented by using the local turbulent kinetic energy and random number generator. The Gaussian probability distribution function is used to define the fluctuation components of the air velocity [12] as follows :

$$u = \bar{u} + u'$$

and

$$u' = \varphi \sqrt{(3/2) k}$$

$$\varphi = [2 \ln (1 / Rn)]^{0.5}, Rn \text{ is random number from random number generator between } (0.001 \text{ to } 1)$$

Initial and Boundary Conditions

The initial velocity of air and fuel issued from the nozzle is calculated as a function of pressure drop across the orifice of air and fuel respectively.

$$u_f = \sqrt{\frac{2(P_f - P_o)}{\rho_f}}$$

$$u_a = \sqrt{\frac{2(P_a - P_o)}{\rho_a}}$$

$$\dot{m}_f = C_d \rho_f u_f A_n$$

A_n is the effective fuel nozzle area

C_d is the coefficient of discharge = 0.75

The amount of fuel injected during the time interval is used for calculating the initial size distribution of the droplets after the breakup process.

$$m_f = \int \dot{m}_f d\tau = \sum n_i \frac{\pi}{6} D_i^3 \rho_f$$

The droplets size distribution D_i and the number of droplets in the same size group n_i can be obtained from the probability distribution function. In the present work Tanaswa and Tesima (T-T) [19] distribution function is used.

Breakup Length

In twin fluid atomizer, the breakup mechanism is somewhat complicated than that of the solid injection. Special technique [4] is used to define the solid core length. The method depends on calculating the breakup length [13] for the solid injection only at first. Modification is made to correct the value of the breakup length according to the air stream effect as follows.

if $Oh > 740 Re^{-1.22}$

then $\tau_b = 375000 / (d_o^{0.28} \rho_a^{0.05} \Delta P^{1.37})$

$$I_o = 2.9 [(\Delta P / \rho_g)^{0.5} d_o \tau_b]^{0.5}$$

$$I_b / I_o = We^{0.0075} Re^{0.5} \text{Exp}(-0.0143 Re^{0.5})$$

Operating Conditions

The proposed mathematical model was used to simulate the atomization process for the twin fluids atomizer with different operating conditions. Table 1 shows these conditions as follows:-

Table 1 : Operating conditions for the prediction model

Run number	P_{air} (bar)	P_{back} (bar)	P_f (bar)	T_f (°C)
1	1.5	1	1.1	90
2	1.5	1	1.4	90

RESULTS AND DISCUSSION

The proposed mathematical model is used to study the spray characteristics of the twin fluid atomizer with heavy liquid fuel. Parametric study has been carried out with different operating conditions. Comparison is held also with experimental

data to validate the assumptions of the mathematical model. Fig. 10 and Fig. 11 represent the spray droplets pattern. From this figure it is clear that the effect of the gas phase turbulence on the droplets dispersion appears on the smallest droplets than that of the big one. The heavy droplets tends to be in the spray core. The momentum of the big droplets increase their ability to penetrate the turbulence eddies without noticeable effect. For this reason the dispersion of droplets resultant from the flow turbulence effect is concentrated mainly upon the smaller size of the droplets. It can be seen from these figures the effect of the fuel pressure on the spray cone angle. Increasing the fuel pressure, the droplets tend to be smaller. The slip velocity between the air and droplets decreased, so the smaller droplets takes a higher angular momentum and consequently higher centrifugal force. This leads to increase spray cone angle. Fig. 12 represents the velocity vectors of the air pattern. From this figure; it is clear that the air velocity takes its maximum value along the spray centerline. The highest value of the entrained air velocity in the spray zone lies near the injector and reaches its maximum value at the spray tip. This may be attributed to the small momentum exchange. Fig. 13 represents the comparison between theoretical and experimental data for the fuel concentration along the spray centerline. The comparison shows a fair agreement, specially near the spray tip. While in the middle zone, the prediction gives an over estimation than the experimental data. This can be attributed to the absence of the droplets collision simulation from the mathematical model.

CONCLUSION

It is clear from the experimental data the great effect of the fuel properties as well as the operating conditions on the spray droplets size represented by D_{32} . Also the correlation which define D_{32} is obtained.

An improved mathematical model is used taking into consideration more accurate initial and boundary conditions. Breakup length and interaction mechanism. The comparison with the experimental data shows a fair agreements.

REFERENCES

1. Rizk, N.K. and Lefebvre, A.H. " Spray Characteristics of Plain Jet Air blast Atomizer", Trans. ASME J. of Power, Vol. 106, pp. 634, 1984.
2. Daniel, L.B. , Yeshayahu, L. , Suresh, K.A. and Susheed C. , "Measurements and Predictions of Liquid Spray From An Air Assist Nozzle", Atomization and Sprays, Vol. 2, No. 4, pp. 445, 1992.
3. Bachalo, W.D. and Houser, M.J. , "Development of the Phase Doppler Spray Analyzer For Liquid Drop Size and Velocity Characterizations", AIAA, 1984.
4. Kim, D.J. and Lee, C.W. , "Behaviour of Surface Waves On the Breakup Mechanism of Liquid Column", ICLASS, pp. 109-204, 1991.
5. Chen, X.A. and Pereira, J.C.F. , "Numerical Prediction of Nonevaporating and Evaporating Fuel Sprays Under Non reactive Conditions", Atomization and Sprays Vol. 2, No. 4, pp. 427, 1992.
6. Solomon, A.S.P., "A theoretical And Experimental Investigation of Turbulent Sprays", Ph.D. thesis, Pennsylvania Stat University, May, 1984.

7. Gosman, A.D. and Ioannides, E. , "Aspects of Computer Simulation of Liquid Fuel Combustors", AIAA, No. 81-0323, 1981.
8. Shuen, J.S., Chen,L.D. and Faeth,G.M., "Predictions of The Structure of Turbulent Particle-Laden Round Jets", AIAA, Vol. 21 , No. 11, pp.1483, 1983.
9. Shuen, J.S. , Chen, L.D. and Faeth, G.M. , "Evaluation of Stochastic Model Of Particle Dispersion In Turbulent Round Jet" , AIChE, Vol. 29, No. 1, 1983.
10. Anderson, O.L. , Chiappetta, L.M., Edwards, DE. and McVey, J.B. , "Analytical Modeling Of Operating Characteristics Of Premixing-Preevaporizing Fuel-Air Mixing Passages", Report No. UTRC 80-102, Vol. I, United Technologies Research Center, East Hartford, Conn., 1980.
11. Yuu,S., Yasukouchi, N. , Hirosawa, Y. and Jotaki, T., "Particle Turbulent Diffusion In A Dust Laden Round Jet", AIChE, Vol. 24, pp. 509, 1978.
12. Elkotb, M.M. , Elbahar, O.M.F. , Sabry, T.I. and Wilson, S.A. , "Droplet Interaction In Spray Modeling", ICLASS 91, pp.753, 1991.
13. Yule, A.J. and Filipovic, I. , "On The Breakup Times And Lengths Of Diesel Spray", Spray & Aerosol, University of Surrey, UK., 1991.
14. Van Doormaal, J.P. and Raithby, G.D. , Numerical Heat Transfer, Vol. 7, PP.147-163, 1984.
15. Viropoff, D.N., "Evaporation of Fuel Drops", Bull. of the Central Scientific Aviation Institute, Vol. 3, 1939.
16. Ranz, W.E. and Marshall , W.R. "Evaporation From Drops" , Part I and II , Chem. Eng. Prog. , Vol. 48, pp.141, 1952.
17. El-Wakil, M.M. , Uyehara, D.A. and Myers, P.S.A. "Theoretical Investigation of The Heating Up Period Of Injected Fuel Droplets Vaporizing In Air", NACA , TN. 3179, 1954.
18. Adler, D. and Lyn, L.T. , "The Steady Evaporation And Mixing Of A Spray In A Gaseous Swirl" , Int. J. Heat & Mass Transfer , Vol. 14, pp. 793, 1971.
19. Tanasawa, Y. and Tesima, T. "On The Theory Of Combustion Rate Of Liquid Fuel Spray", Bull. Of JSME , 1958.

NOMENCLATURE

A	Droplet surface Area	m ²	H	Enthalpy	J
AF	Air to fuel ratio.		I	Breakup length	m
C _D	Drag coefficient.		K	Thermal conductivity	w/m K
C _p	Specific heat	j/kg K	L	Latent heat of fuel	j/kg
D _c	Diffusion coefficient		m _r	Local fuel mass concentration	kg
D _i	Droplet diameter in the size group i	m	Nu	Nusselt number	
d ₀	Fuel nozzle diameter	m	n _i	Number of droplets in size group i	
d _L	Droplet diameter	m	Oh	Ohnesorge number	
D ₃₂	Sauter mean diameter	m			
h	Coefficient of heat transfer	w/m ² K			

$= \mu_L / \sqrt{\sigma_{1\rho_L d_0}}$

P	Pressure	Pa	We	Weber number	
Pr	Prandtle number		α	Void fraction.	
R	Droplet's radius	m	Γ_{ϕ}	Effective diffusivity	
Re	Reynolds number			coefficients for variable ϕ	
R_v	Vapour gas constant	j/kg K	k	Turbulent kinetic energy	m^2/s^2
Sc	Schmidt number		μ	Dynamic viscosity	Pa.s
Sh	Sherwood number		ρ	Density	kg/m^3
T	Temperature	K	σ	Surface tension	N/m
t	Temperature	$^{\circ}C$	τ	Time	sec
U, V, W	Velocity components in x, y, z directions respectively.	m/s	τ_{ij}	Shear stress	N/m^2
			ϵ	Energy dissipation rate	m^2/s^3

Subscripts

A	Air	v	Vapour
e	Eddies	R	Relative
g	Gas	r	Residence
L	Liquid	int	Interaction
o	Initial	b	Breakup
s	Separation		

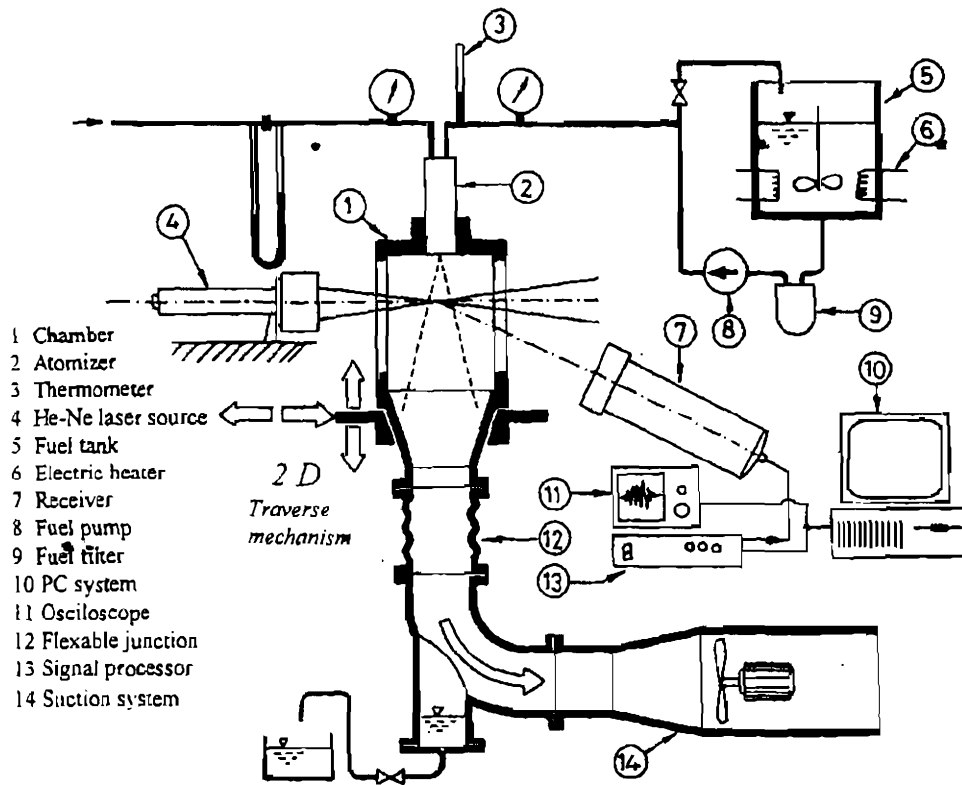


Fig.1 Details of experimental test rig.

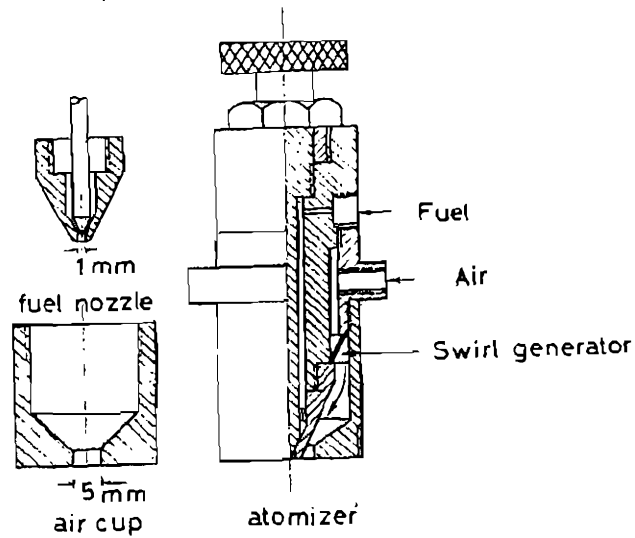


Fig.2 Details of the twin fluid atomizer.

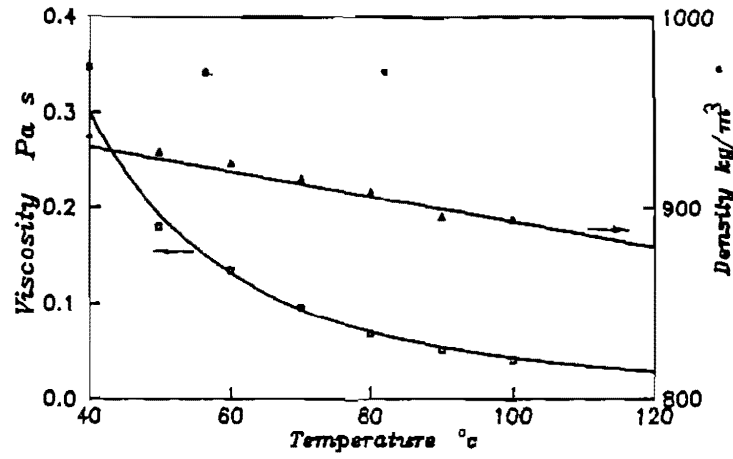


Fig.3 Fuel viscosity and density gradients with respect to temperature.

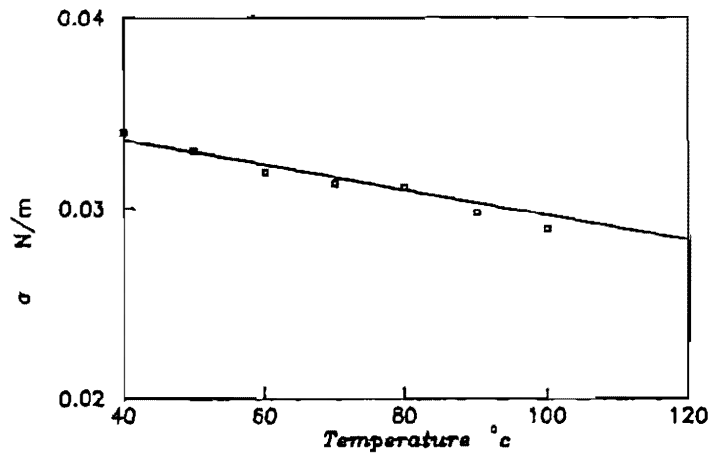
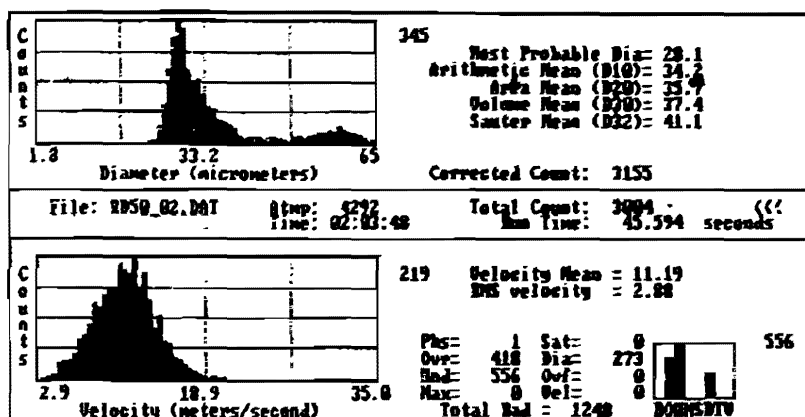


Fig.4 Variation of surface tension of the fuel with respect to temperature.



Axial distance = 14 cm
 Radial distance = 1 cm

Fig. 5 Typical output results from the P/DPA system.

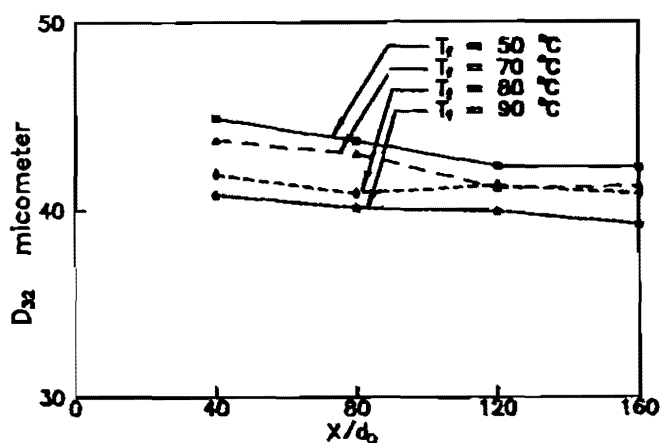


Fig. 6 Spatial distribution of the droplets size along the spray axis.

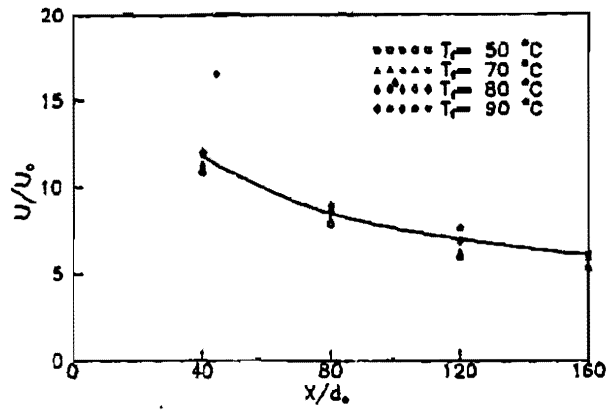


Fig. 7 Droplets velocity along the spray axis.

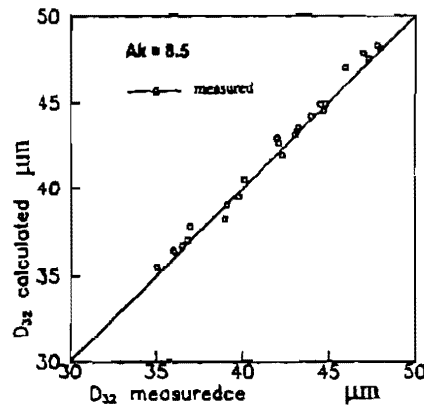


Fig. 8 Comparison of calculated and measured values of mean drop size.

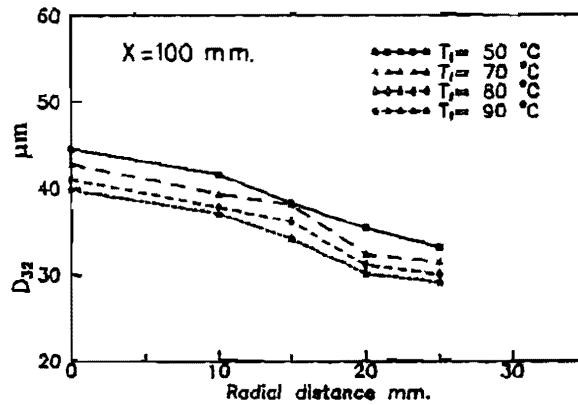


Fig. 9 Radial droplets size distribution.

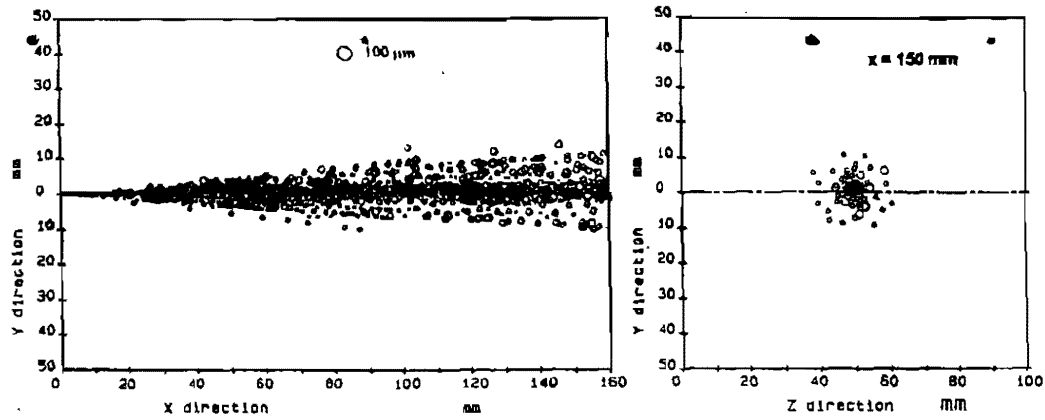


Fig. 10 Spray droplets pattern at ,
 $P_f=1.1$ bar , $P_{air}=1.5$ bar , $P_o=1$ bar

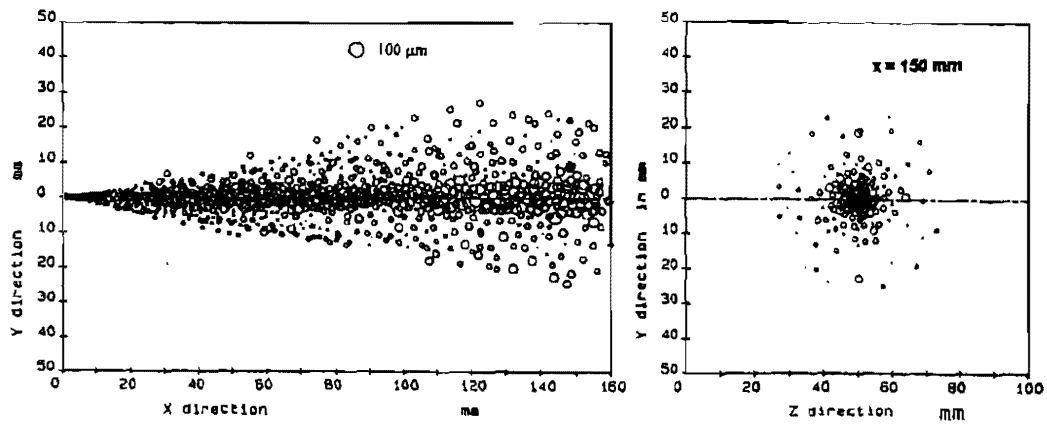


Fig. 11 Spray droplets pattern at ,
 $P_f=1.4$ bar , $P_{air}=1.5$ bar , $P_o=1$ bar

Velocity vector scale 3 m/s per 1 mm.

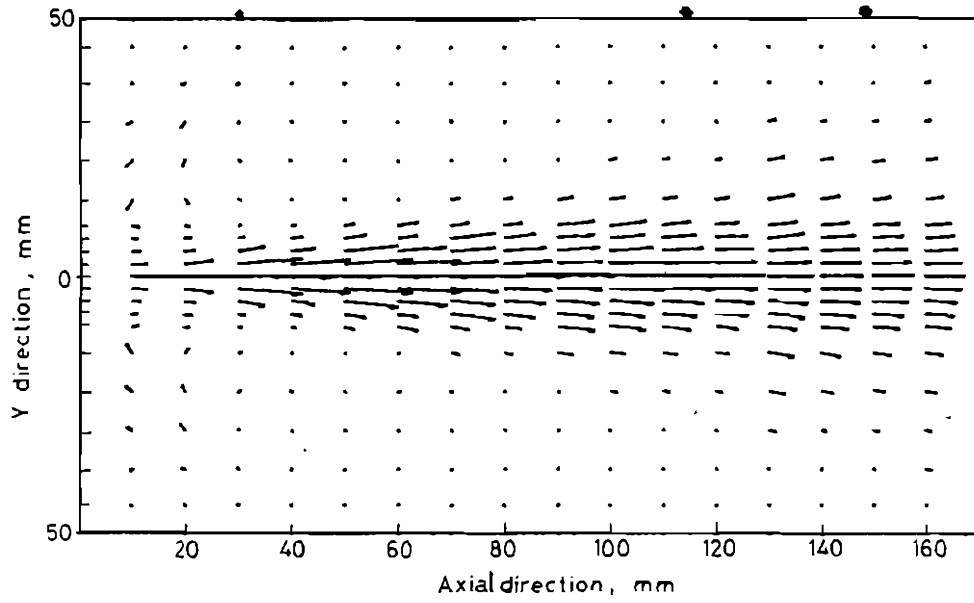


Fig. 12 Velocity vector of the gas phase
(Air jet velocity 65 m/s)

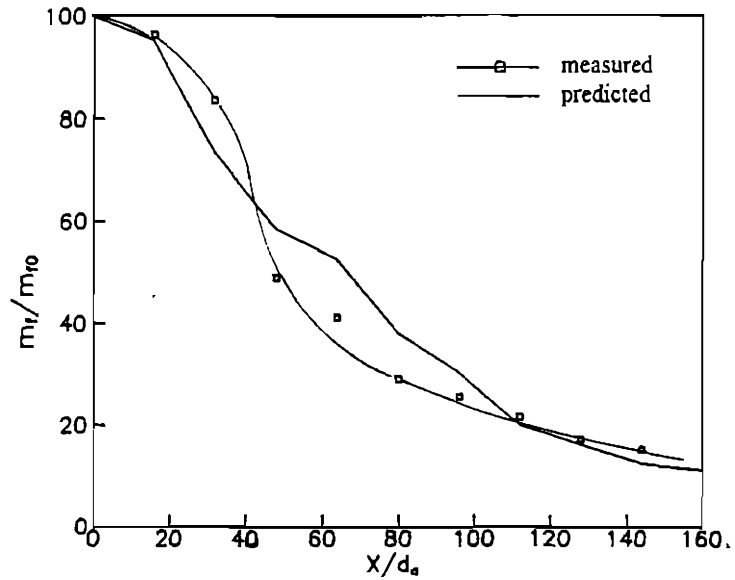


Fig. 13 Decay of axial fuel concentration
 $P_f=1.1$ bar, $P_{air}=1.5$ bar, $P_o=1$ bar, $T_f=90^\circ\text{C}$